Eur. Phys. J. AP **18**, 189–200 (2002)
DOI: 10.1051/epjap:2002040

THE EUROPEAN PHYSICAL JOURNAL
APPLIED PHYSICS

Boltzmann equation and Monte Carlo analysis of the spatiotemporal electron relaxation in nonisothermal plasmas

D. Loffhagen[1,a], R. Winkler[1], and Z. Donkó[2]

[1] Institut für Niedertemperatur-Plasmaphysik, Friedrich-Ludwig-Jahn-Str. 19, 17489 Greifswald, Germany
[2] Research Institute for Solid State Physics and Optics, PO Box 49, 1525 Budapest, Hungary

Received: 7 February 2002 / Received in final form: 12 April 2002 / Accepted: 23 April 2002
Published online: 6 June 2002 –

Abstract. The spatiotemporal relaxation of electrons in spatially one-dimensional plasmas acted upon by electric fields is investigated on the basis of the space- and time-dependent electron Boltzmann equation. The relaxation process is treated using the two-term approximation of an expansion of the electron velocity distribution function in Legendre polynomials. To verify the complex Boltzmann equation approach by a completely independent kinetic method, results for inhomogeneous column-anode plasmas of glow discharges between plane electrodes are compared with corresponding ones obtained by Monte Carlo simulations. The spatiotemporal electron relaxation in argon plasmas, subjected to a space-independent electric field and maintained by a time-independent inflow of electrons at the cathode side of the plasma region, is considered. Starting from steady state at a given electric field, the relaxation process is initiated by a pulse-like change of the electric field strength and is traced until the spatially structured, time-independent state associated to the changed field is reached. The behaviour of the velocity distribution function and macroscopic quantities of the electrons in space and time is analyzed for enlarged and reduced electric field strengths typical of the column region of glow discharges. In particular, the spatiotemporal reformation of plasma structures has been found to progress in two phases, *i.e.*, existing structures in the distribution are driven to merge in wide plasma region first, followed by a formation phase of new spatial structures which are induced by the cathode-sided inflow of electrons. The results for the macroscopic quantities and the isotropic distribution functions obtained by Boltzmann and Monte Carlo calculations agree very well during the spatiotemporal transient process as well as in the new steady state finally reached.

PACS. 52.25.Dg Plasma kinetic equations – 52.65.Pp Monte Carlo methods – 51.50.+v Electrical properties (ionization, breakdown, electron and ion mobility, etc.)

1 Introduction

The study of the spatiotemporal relaxation of nonisothermal, collision-dominated plasmas under the action of an electric field constitutes a topic of widespread interest. Relaxation processes are related, for example, to afterglow decay, swarm techniques, pulsed discharges for plasma light generation and problems of plasma processing.

For the physical understanding of the spatiotemporal relaxation of these plasmas the behaviour of the electron component is of particular importance, since the electrons energetically feed the other plasma components. The power input to the plasma frequently takes place by the injection of electrons in the presence of an electric field or by an electron beam. Then, this power input is transferred to the heavy particles by elastic and different types of inelastic electron collision processes, leading to drastic changes in the concentrations of various heavy particle components. This interplay between power input and power dissipation in collisions causes the electron component to usually be far from the equilibrium with the instantaneous or local field in different stages of the relaxation process. Thus, the nonequilibrium behaviour of the electron component in nonisothermal plasmas can only be described on an appropriate microphysical basis.

In principle, two quite different approaches can be applied to microphysical studies of the behaviour of the electrons. One of the approaches consists of the solution of the electron Boltzmann equation. So far, the treatment of this kinetic equation is widely restricted to time-dependent, but spatially homogeneous plasmas [1–6] or to space-dependent, but stationary plasmas [7–17]. In recent years the spatiotemporal description of the kinetics of electrons in spatially one-dimensional plasmas [18–20] became possible, too. As a particular result of these latter studies, it became evident that the physics of the spatiotemporal

[a] e-mail: loffhagen@inp-greifswald.de

behaviour of the electrons differs substantially from that of the purely time-dependent evolution in spatially uniform plasmas. Thus, there is a basic necessity for a profound analysis of the spatiotemporal behaviour of the electron component, in order to obtain a deeper understanding of the physics involved.

The other approach uses the techniques of particle simulation. Particle simulations have extensively been applied to study particle transport under swarm conditions as well as different types of DC and RF discharges, *e.g.* in [21–30]. The simulation technique has the advantage that it can easily be applied to more complicated geometries than the solution approach of the kinetic equation. However, it is generally time consuming, since a large number of electrons has to be treated in any simulation to get a sufficient statistical resolution and thus accuracy for the determination of *e.g.* the velocity distribution of the electrons in the region of higher electron energies where the inelastic collision processes occur. The treatment of the kinetic equation does usually not possess this limitation and its computational expenditure is generally comparatively low. Nonetheless, particle simulation techniques become more and more adequate to microphysical studies because of the continuous increase of computational power.

In the present paper, both these techniques have been adopted to investigate the spatiotemporal relaxation of the electron component in the column-anode plasma region of glow discharges between plane electrodes. The plasma is acted upon by an electric field and sustained by a continuous inflow of electrons at its cathode side. In particular, the spatiotemporal reformation of spatial plasma structures in the axial direction caused by an abrupt change of the electric field strength has been analyzed.

The time-dependent, spatially one-dimensional Boltzmann equation of the electrons has been solved by means of the recently developed method reported in [20]. It is based upon the two-term approximation of the velocity distribution function expansion in Legendre polynomials and the quasi-stationary description of the anisotropic part of the distribution. In order to verify the complex treatment of the electron kinetic equation, the same relaxation problem has been dealt with by means of Monte Carlo simulations. The comparison of results obtained by both approaches has been performed for electric fields typical of the column region of glow discharges. It concerns the isotropic and anisotropic part of the velocity distribution function as well as selected macroscopic quantities of the electrons.

The investigations are mainly aimed to elucidate the physics involved in the spatiotemporal behaviour of plasmas and to verify the two-term approach of the electron Boltzmann equation. On the other hand, the comparison of the different kinetic approaches is meant to give a feeling with respect to the performance of both techniques. In particular, the applicability of Monte Carlo simulations to studies of the space- and time-dependent evolution of electrons is evaluated.

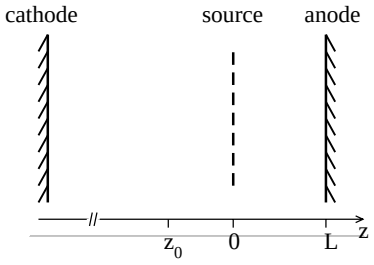

Fig. 1. Idealized arrangement of the plasma region between plane electrodes.

2 Theoretical foundations

In order to perform comparative investigations of the spatiotemporal electron relaxation by means of the solution of the electron Boltzmann equation and Monte Carlo simulations, the specific relaxation process has to be defined carefully. The various space- and time-dependent relaxation processes which can be described by the kinetic approaches can differ from each other by the imposed conditions, for example, the density, temperature and atomic data of the background gas, the electric field strength as well as the initial values and boundary conditions.

In the present studies the conditions are chosen to resemble the column-anode plasma region of low pressure glow discharges between plane electrodes. The simplified plane-parallel geometry is shown in Figure 1. The spatial variation of the plasma occurs only along the z axis. A main task regarding the comparison of Boltzmann and Monte Carlo calculation results consists in the adaptation of correlated boundary conditions and initial values. In the framework of the present relaxation model a continuous inflow of electrons at the cathode side of the plasma region, *i.e.*, at the position $z = 0$, takes place. In Boltzmann equation studies the influx of electrons into a plasma region is naturally determined by prescribing the anisotropic part of the velocity distribution [20,31] and no information about the isotropic part of the velocity distribution is required. The direct transfer of this description to the Monte Carlo approach is not possible. Instead, the inflow of electrons at the position $z = 0$ is assumed to come from a source releasing electrons with a constant rate R_S. For these electrons an isotropic angular distribution has been adopted. The energetic distribution of the released electrons is chosen to equal the Gaussian function

$$G(U) = \exp\left[-\left(\frac{U-U_\mathrm{c}}{U_\mathrm{w}}\right)^2\right] \times \left(\int_0^{2U_\mathrm{c}} \exp\left[-\left(\frac{U-U_\mathrm{c}}{U_\mathrm{w}}\right)^2\right] \mathrm{d}U\right)^{-1} \quad (1)$$

in the range from 0 to $2U_\mathrm{c}$. The parameters of the Gaussian distribution are the centre energy U_c and the energy width U_w.

The electrons are subjected to the spatially uniform electric field $\boldsymbol{E} = E(t)\boldsymbol{e}_z$. To allow the acceleration of the

electrons in the positive z direction toward the anode, E is assumed to be negative everywhere. The anode is situated at the position $z = L$, where $L = 10$ cm has been employed for the calculations. The electrons reaching the anode are assumed to be partially reflected. The additional effect of an anode fall has not been taken into account.

Because of the electron source and of collisions of electrons with neutral background gas particles, there is a certain number of electrons in the region of $z < 0$ as well. These electrons are also accelerated by the electric field action toward the anode, so that sufficiently far away from the source no electrons exist in the region $z < z_0$.

To start the spatiotemporal relaxation process from well-defined initial conditions, first the spatially structured, steady state at a given electric field has been determined by means of the solution of the electron Boltzmann equation and Monte Carlo simulations. Then, the spatiotemporal electron relaxation is triggered by an instantaneous change of the electric field strength, while keeping the continuous inflow of electrons at the cathode side of the plasma region unchanged. The reformation of the spatial plasma structures in space and time is traced until approaching the spatially structured, steady state associated with the changed field.

In the following, main aspects of the treatment of the kinetic equation of the electrons and of the Monte Carlo simulations are reported.

2.1 Boltzmann equation approach

Starting point for the analysis of the spatiotemporal electron relaxation in nonisothermal, collision-dominated plasmas is the space- and time-dependent Boltzmann equation of the electrons

$$\frac{\partial}{\partial t}F + \boldsymbol{v}\cdot\nabla_{\boldsymbol{r}}F - \frac{e_0}{m_e}\boldsymbol{E}\cdot\nabla_{\boldsymbol{v}}F = C^{\mathrm{el}}(F) + \sum_m C_m^{\mathrm{in}}(F) + \tilde{P}_{\mathrm{S}}, \tag{2}$$

where $F(\boldsymbol{r},\boldsymbol{v},t)$ denotes the velocity distribution function of the electrons with the charge $-e_0$ and the mass m_e and $\boldsymbol{r}$, $\boldsymbol{v}$ and t are the space position, velocity and time, respectively. C^{el} and C_m^{in} represent the collision integrals for the elastic and the various (m) inelastic collision processes of electrons with background gas particles, respectively. For simplicity in the further representation, only inelastic collision processes conserving the electron number are taken into account in the kinetic treatment. In addition, the right-hand side of equation (2) includes the term $\tilde{P}_{\mathrm{S}}$ describing the effect of a source of electrons.

Considering a spatially inhomogeneous plasma with the plasma inhomogeneity in the direction of the electric field, *i.e.*, parallel to the z direction, the velocity distribution function becomes symmetrical around the field and gets the reduced dependence $F(z,U,v_z/v,t)$ on the space coordinate z, the kinetic energy $U = m_e v^2/2$ with the velocity magnitude $v = |\mathbf{v}|$, the direction cosine v_z/v and the time t. Thus, the velocity distribution function can be given an expansion in Legendre polynomials, which gets the representation

$$F(z,U,v_z/v,t) = \frac{1}{2\pi}\left(\frac{m_e}{2}\right)^{3/2} \times \left(f_0(z,U,t) + \frac{v_z}{v}f_1(z,U,t)\right) \tag{3}$$

in the lowest approximation order, the so-called two-term approximation. When substituting this expansion and the relation

$$\tilde{P}_{\mathrm{S}}(z,U) = \frac{1}{2\pi}\left(\frac{m_e}{2}\right)^{3/2} U^{-1/2} P_{\mathrm{S}}(z,U) \tag{4}$$

into the Boltzmann equation (2) and when additionally adopting the widely used assumption that the temporal evolution of the anisotropic part $f_1(z,U,t)$ of the velocity distribution function takes place in a quasi-stationary way with respect to the temporal evolution of the isotropic part $f_0(z,U,t)$ of the velocity distribution function and of the electric field $E(t)$, finally the three-dimensional partial differential equation [20]

$$\begin{aligned}
&\left(\frac{m_e}{2}\right)^{1/2} U^{1/2}\frac{\partial}{\partial t}f_0 - \frac{\partial}{\partial z}\left[\frac{1}{3}\frac{U}{NQ^d(U)+\sum_m NQ_m^{\mathrm{in}}(U)} \times\left(\frac{\partial}{\partial z}f_0 - e_0E(t)\frac{\partial}{\partial U}f_0\right)\right] \\
&+\frac{\partial}{\partial U}\left[\frac{1}{3}\frac{Ue_0E(t)}{NQ^d(U)+\sum_m NQ_m^{\mathrm{in}}(U)} \times\left(\frac{\partial}{\partial z}f_0 - e_0E(t)\frac{\partial}{\partial U}f_0\right)\right] \\
&-\frac{\partial}{\partial U}\left(2\frac{m_e}{M}U^2NQ^d(U)f_0\right) + \sum_m UNQ_m^{\mathrm{in}}(U)f_0 \\
&-\sum_m \left(U+U_m^{\mathrm{in}}\right)NQ_m^{\mathrm{in}}\left(U+U_m^{\mathrm{in}}\right)f_0\left(z,U+U_m^{\mathrm{in}},t\right) \\
&-\left(\frac{m_e}{2}\right)^{1/2} P_{\mathrm{S}}(z,U) = 0
\end{aligned} \tag{5}$$

for the isotropic distribution $f_0(z,U,t)$ results. Here N and M denote the density and mass of the background gas particles assumed to be at rest. Q^d and Q_m^{in} are the cross sections for momentum transfer in elastic collisions and for the mth inelastic collision process with the energy loss U_m^{in}. On deriving equation (5) a truncation of each collision integral after the leading term of a further expansion with respect to the ratio m_e/M of electron to gas particle mass has been performed. As usual, the scattering processes associated with the inelastic collisions are assumed to be isotropic, while arbitrary scattering in elastic collisions is considered [32,33]. The isotropic source function $P_{\mathrm{S}}(z,U)$ describing the continuous inflow of electrons at $z = 0$ is specified by the relation $P_{\mathrm{S}}(z,U) = R_{\mathrm{S}}G(U)h(z)$ with $h(z) = 1$ close to $z = 0$ and $h(z) = 0$ elsewhere.

Equation (5) determines the evolution of the isotropic part $f_0(z,U,t)$ of the velocity distribution in the space of the coordinate z, the kinetic energy U of the electrons and the time. After the abrupt field variation the isotropic distribution changes in time because of the overlapping impact of the spatially varying electron motion, the electron

acceleration in the electric field, the injection of electrons by the source and different binary collision processes of electrons with neutral background gas particles.

As regards the temporal evolution of the anisotropic part $f_1(z,U,t)$ of the velocity distribution, a quasi-stationary description is applied. Thus, the spatiotemporal behaviour of the anisotropic distribution is determined by that of the isotropic distribution according to the relation

$$f_1(z,U,t) = -\frac{1}{NQ^d(U)+\sum_m NQ_m^{\mathrm{in}}(U)} \times \left(\frac{\partial}{\partial z}f_0(z,U,t) - e_0E(t)\frac{\partial}{\partial U}f_0(z,U,t)\right). \quad (6)$$

Almost all relevant macroscopic quantities of the electrons can be obtained by appropriate energy space averaging over the isotropic and anisotropic distribution functions. Thus, the determination of the spatiotemporal behaviour of the isotropic and anisotropic distribution makes it possible to calculate the spatiotemporal evolution of *e.g.* the density $n_e(z,t)$, the mean energy $u_m(z,t)$, particle flux density $\boldsymbol{j}(z,t) = j_z(z,t)\boldsymbol{e}_z$ and the energy flux density $\boldsymbol{j}_e(z,t) = j_{ez}(z,t)\boldsymbol{e}_z$ of the electrons. The first two quantities are obtained by energy space averaging over the isotropic distribution $f_0(z,U,t)$, while the latter two are averages of the anisotropic distribution $f_1(z,U,t)$. They have the representation

$$n_e(z,t) = \int_0^\infty U^{1/2}f_0(z,U,t)\mathrm{d}U, \quad (7)$$

$$u_m(z,t) = \frac{1}{n_e(z,t)}\int_0^\infty U^{3/2}f_0(z,U,t)\mathrm{d}U, \quad (8)$$

$$j_z(z,t) = \frac{1}{3}\left(\frac{2}{m_e}\right)^{1/2}\int_0^\infty Uf_1(z,U,t)\mathrm{d}U, \quad (9)$$

$$j_{ez}(z,t) = \frac{1}{3}\left(\frac{2}{m_e}\right)^{1/2}\int_0^\infty U^2f_1(z,U,t)\mathrm{d}U. \quad (10)$$

For the determination of the spatiotemporal relaxation of the electrons in the framework of the two-term approximation and the quasi-stationary description of the anisotropic distribution, equation (5) has been solved. The powerful technique for the solution of this equation for the isotropic distribution f_0 in high accuracy has been described in detail in [20]. A brief representation of main aspects of the solution technique follows.

The natural solution region of the relaxation problem is the region ($z_0 \le z \le L,\ 0 \le U \le U_\infty,\ t \ge 0$), where $z = z_0$ and $z = L$ are the spatial margins and U_∞ is an appropriate upper limit of the kinetic energy above which the isotropic distribution becomes negligibly small. In order to solve equation (5), a transformation from the kinetic energy U to the total energy $\varepsilon = U + W(z)$ with the potential energy $W(z) = e_0E(z - z_0)$ has been performed. The resulting three-dimensional partial differential equation for the transformed isotropic distribution is numerically solved as an initial-boundary value problem over the space of the spatial coordinate z and the total energy ε proceeding in time. For the solution appropriate boundary conditions in space and energy have to be given. In particular, at the spatial margin $z = z_0$ the isotropic distribution equals zero, since sufficiently far away from the source no electrons exist in the region of $z \le z_0$. At the anode, located at $z = L$, a condition characterizing the absorption and partial reflection of electrons has to be adopted. In accordance with the literature [15] it is assumed that the anisotropic distribution at the anode is proportional to the isotropic distribution with a constant of proportionality describing the fraction of reflection.

The numerical solution of the partial differential equation for the transformed isotropic distribution has been obtained by using a finite difference approximation on a three-dimensional grid in the (z,ε,t) space. The discretization has been done on an equidistant grid in space, total energy and time and the discrete form of the partial differential equation has been derived using second-order-correct difference analogues for the transformed distribution function and its partial derivatives following the Crank-Nicolson scheme with respect to time. For each time step a parabolic equation with regard to ε results and the discrete representation of this equation has been solved in the (z,ε) plane by using the powerful tridiagonal algorithm [34], where a progression of the solution from higher to lower total energies has been found to be favourable. Typically, an energy step size $\Delta\varepsilon$ of 0.05 eV and a corresponding step size $\Delta z = \Delta\varepsilon/(e_0|E|)$ of the space coordinate have been employed for the calculations reported below in this paper. The time step sizes Δt ranged between 0.01 (at the beginning of the relaxation) and 1 ns. Several thousand time steps were necessary to approach the new spatially structured steady state [20]. To determine the relaxation behaviour up to steady state for a given situation, a computing time of less than half a day was required using a 400 MHz processor of a Silicon Graphics Origin 2000 server.

2.2 Monte Carlo approach

Monte Carlo simulations of the spatiotemporal relaxation processes have also been performed with the intention to confirm or to find possible limitations of the two-term approach adopted for the solution of the Boltzmann equation. In the Monte Carlo simulation the trajectory of each electron between collisions has been obtained by the simultaneous, numerical integration of the equation of motion of the electrons

$$\frac{\mathrm{d}^2\boldsymbol{r}}{\mathrm{d}t^2} = -\frac{e_0}{m_e}\boldsymbol{E} \quad (11)$$

and the equation assigning the length of the free flight

$$\int_{s_0}^{s_c} NQ^T(U(s))\mathrm{d}s = -\ln(1-R_{01}), \quad (12)$$

where $Q^T(U) = Q^d(U) + \sum_m Q_m^{\mathrm{in}}(U)$ is the energy-dependent total cross section of electron collisions with

the gas particles, s_0 and s_c denote the position of the free flight start and that of the next collision measured on the curvilinear path s along the trajectory and R_{01} is a random number uniformly distributed between 0 and 1. Owing to the assumption that the electric field acts parallel to the z direction (*i.e.*, perpendicular to the plane electrodes), the electron motion becomes symmetrical around the field and the study of the electron motion reduces to the phase space $(z, U, v_z/v, t)$ (see *e.g.* [35]). Sequences of random numbers are used as well to determine (i) the type of collision process that occurred after a free flight, taking into account the cross section values of the different collision processes at the energy of the colliding electron, and (ii) the change of velocity direction during a collision [36].

A second-order Runge-Kutta method has been used for the simultaneous time integration of equations (11, 12). This method has been found to represent a good compromise between accuracy and computational speed. It provides sufficient accuracy, where a time step of 5 ps has typically been employed. Further simulations have been done using a fourth-order Runge-Kutta method. These simulations confirmed the results obtained by the second-order Runge-Kutta method at nearly doubled computing time. Two independent simulation codes written in different languages by different authors and executed on different computers provide additional confidence in the reliability of the Monte Carlo results.

The electron velocity distribution function and related macroscopic quantities have been determined during the Monte Carlo simulation. Details about appropriate sampling methods can be found in the literature (see *e.g.* [37,38]). In the present paper results for the isotropic part f_0 and the anisotropic part f_1 of the velocity distribution function as well as for related macroscopic quantities, namely the density, mean energy and the particle and energy flux density of the electrons, are represented. Several tests have been carried out to determine the adequate energy resolution and appropriate time and space intervals. The results shown below have usually been obtained with the sampling intervals $\Delta U_{\mathrm{MC}} = 0.5$ eV, $\Delta t_{\mathrm{MC}} = 0.1$ μs and $\Delta z_{\mathrm{MC}} = 0.05$ cm. These values provide a good statistics while ensuring that no spatial or temporal structures are significantly smeared. To allow the comparison between Monte Carlo and Boltzmann calculation results of the velocity distribution function over about five orders of magnitude, several months of computing time on one 400 MHz processor of a Silicon Graphics Origin 2000 server are needed to determine the entire spatiotemporal relaxation behaviour at a typical situation reported in this paper. The use of a null-collision technique [21] could reduce the computational expenditure of the Monte Carlo calculations, but to a limited extent only.

3 Results and discussion

Boltzmann and Monte Carlo calculations of the spatiotemporal electron relaxation have been performed for argon plasmas at a gas density of $N = 3.54 \times 10^{16}$ cm^{-3} (corresponding to a gas pressure of 1 torr at a temperature of 273 K). The cross sections of electron-argon collision processes recommended by Phelps [39] have been used. The cross section set is shown in Figure 2. It includes cross sections of momentum transfer in elastic collisions, total excitation with the energy loss $U_1^{\mathrm{in}} = 11.5$ eV and ionization with the energy loss $U_2^{\mathrm{in}} = 15.8$ eV. Notice that, for simplicity, in all calculations the ionization process is treated as a conservative inelastic collision process which does not change the electron number in the collision event.

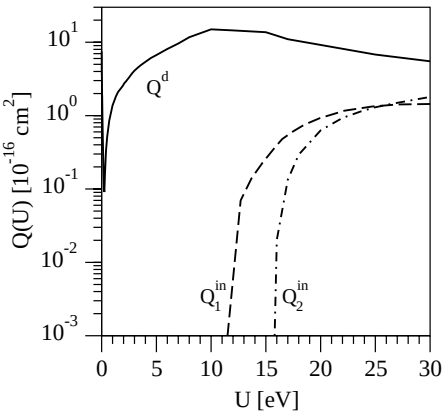

Fig. 2. Collision cross sections for argon.

Within the framework of the relaxation model, column-anode plasma regions acted upon by a constant electric field and sustained by a continuous inflow I_{s} of electrons at the cathode side have been considered. In the Monte Carlo simulations it is assumed that 2000 electrons per square centimeter are released from the source at the position $z = 0$ every nanosecond, *i.e.*, $I_{\mathrm{s}} = 2 \times 10^{12}$ cm^{-2} s^{-1}. This inflow corresponds to a rate of $R_{\mathrm{s}} = I_{\mathrm{s}}/\Delta z_{\mathrm{MC}} = 4 \times 10^{13}$ cm^{-3} s^{-1} in the Boltzmann calculations. The electrons are released isotropically and the centre and width of their energetic distribution (1) have been chosen to be $U_{\mathrm{c}} = 5$ eV and $U_{\mathrm{w}} = 2$ eV. At the anode, *i.e.*, at the position $z = 10$ cm, partial electron reflection with a probability of 36% has been employed.

The calculations of the spatiotemporal electron relaxation for the argon plasma have been performed at various electric field strengths typical of the column region of low pressure glow discharges. Here, results for the spatiotemporal reformation of spatial plasma structures under the action of the two field strengths $E = -6$ and -2 V/cm are presented. The relaxation processes always start from the spatially structured, time-independent state at a given electric field. They are triggered by an instantaneous change of the electric field at the time $t = 0$ and are traced until the spatially structured, new steady state associated with the changed field is reached. The steady state at $E = -2$ V/cm has been used as initial condition for the electron relaxation under the action of the field $E = -6$ V/cm, while the steady state at $E = -6$ V/cm represents the initial condition for the relaxation study at $E = -2$ V/cm. The discussion and

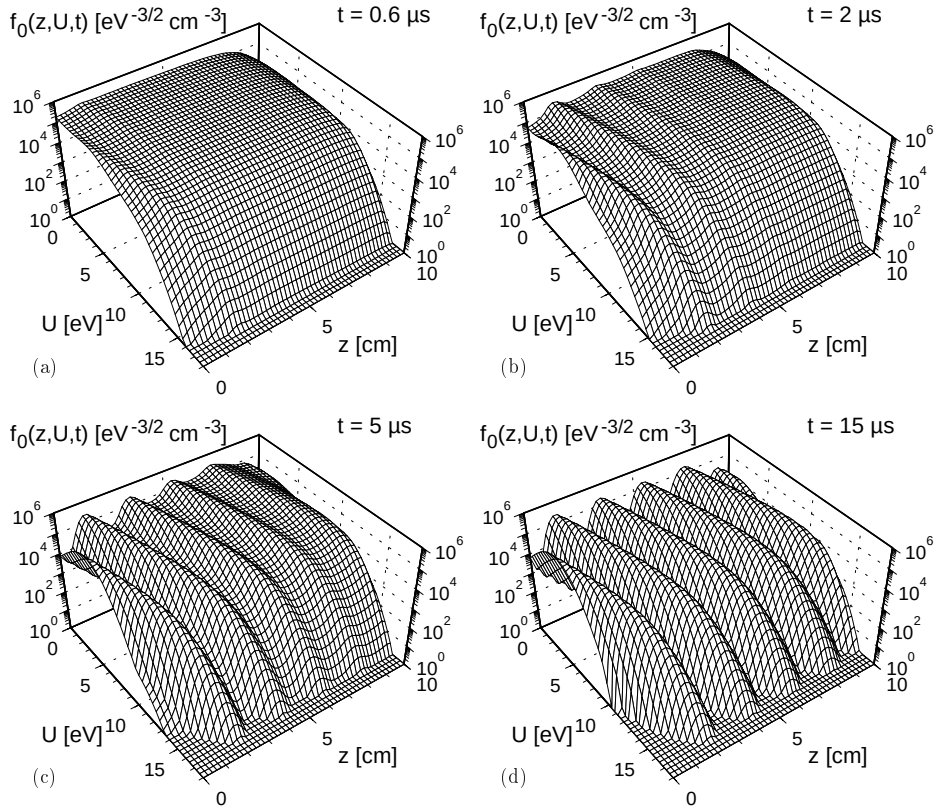

Fig. 3. Isotropic distribution $f_0(z, U, t)$ as a function of the space coordinate z and the kinetic energy U for $E = -6$ V/cm at the times $t = 0.6$ (a), 2 (b), 5 (c) and 15 μs (d).

analysis of the results presented in the following have been performed with respect to the direction of the electron acceleration starting from the electron source, *i.e.*, for the range between $z = 0$ and 10 cm. For the solution of the electron kinetic equation (5) $z_0 = -5$ cm has been used.

In order to illustrate the overall relaxation behaviour, Figures 3a–3d show the spatiotemporal evolution of the isotropic distribution $f_0(z, U, t)$ as a function of the space coordinate z and the kinetic electron energy U at the electric field $E = -6$ V/cm. The spatiotemporal alteration of the isotropic distribution at the electric field $E = -2$ V/cm is represented in Figures 4a–4d. The figures belong to several instants of the transient phase of the relaxation course (Figs. 3a–3c and 4a–4c, respectively) and to the respective established time-independent state (Figs. 3d and 4d). The results have been obtained by the solution of the electron kinetic equation (5).

From these figures main aspects of quite different spatiotemporal relaxation processes can be observed. Starting from the steady state distribution at $E = -2$ V/cm presented in Figure 4d, the sudden change of the electric field to $E = -6$ V/cm at $t = 0$ initiates the relaxation course illustrated in Figure 3. As it can be seen from Figure 3a, the increase of the electric field magnitude and the corresponding increase of the power input from the electric field force the population at higher kinetic energies to grow. The distribution function becomes spatially more homogeneous in wide regions of the plasma when compared with the initial distribution. Close to the cathode side margin the continuous inflow of electrons induces simultaneously the formation of new spatial structures in the distribution function. This new spatial variation spreads from the cathode side towards the anode with increasing time (Figs. 3b and 3c) whereby the structural pattern becomes more and more pronounced. Maintained by the continuous inflow of electrons due to the source at the cathode side, the structures mainly result from the overlapping action of the electron acceleration in the electric field and the backscattering of electrons in their energy space owing to the occurrence of inelastic collision processes of electrons with the argon gas particles. Finally, the strongly structured steady state with a period length of the spatial structures of about 2 cm is reached after about 15 μs (Fig. 3d).

The distribution function of this steady state at $E = -6$ V/cm represents the initial condition of the reverse relaxation process, *i.e.*, the relaxation initiated by the reduction of the magnitude of the field strength. Changing at the time $t = 0$ the electric field abruptly to $E = -2$ V/cm, the relaxation course shown in Figure 4 proceeds. Because the power input from the field is reduced, the high energy part of the distribution function becomes overpopulated. As can be seen from Figure 4a, this overpopulation at higher energies is depleted rapidly as a result of the electron backscattering to lower energies due to inelastic collision processes during the early

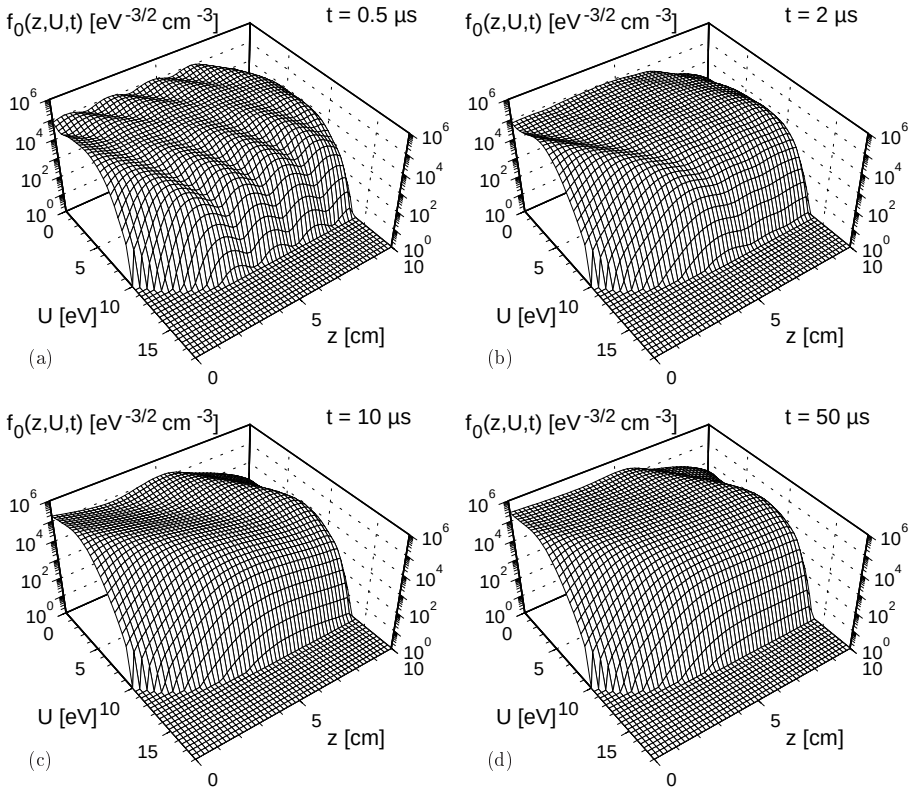

Fig. 4. Isotropic distribution $f_0(z, U, t)$ as a function of the space coordinate z and the kinetic energy U for $E = -2$ V/cm at the times $t = 0.5$ (a), 2 (b), 10 (c) and 50 μs (d).

relaxation course. At the same time the motion of the electrons and the associated transfer of energy lead to a mergence of the initially pronounced structures, while the impact of elastic collisions is relatively weak. In the further course of the relaxation processes, represented by the distributions at the instants 2 and 10 μs (Figs. 4b and 4c), new spatial structures in the distribution function develop at the cathode side, which propagate towards the anode. When approaching the new steady state after about 50 μs, a comparatively weakly structured distribution is obtained (Fig. 4d) as a result of the stronger spatial damping by elastic collisions at the lower electric field strength. In accordance with [40] the period length λ of the resulting spatial structures can be approximated by the quotient of the lowest ground state excitation potential U_1^{in}/e_0 and the magnitude of the electric field E, *i.e.*, $\lambda = U_1^{\mathrm{in}}/(e_0|E|)$, since the potential energy $e_0|E|\lambda$ gained per electron on one period length is almost completely lost in one inelastic collision.

In the following, comparisons between results obtained by the solution of the electron Boltzmann equation and by Monte Carlo simulations are reported. In order to compare the results relevant to the spatiotemporal relaxation of the isotropic distribution function $f_0(z, U, t)$, several instants of the spatiotemporal reformation of spatial plasma structures at $E = -2$ and -6 V/cm are considered. As representatives of the relaxation course, the same points of time as shown in Figures 3 and 4 for the relaxation at $E = -6$ and -2 V/cm, respectively, have been chosen and at each instant the isotropic distribution as a function of the kinetic energy U is represented for different positions z.

Figure 5 shows results belonging to the spatiotemporal relaxation at $E = -6$ V/cm. The lines denote the isotropic distributions obtained by solving the electron Boltzmann equation. The symbols are the corresponding results obtained by Monte Carlo simulations. As one can see, the results of both approaches agree very well during the transient phase of the relaxation course (Figs. 5a–5c) as well as in the pronouncedly structured, time-independent state (Fig. 5d). Similar good agreement is found for the spatiotemporal relaxation of the electrons at the electric field $E = -2$ V/cm, as demonstrated by Figure 6. The comparisons span about five orders of magnitude of the isotropic distribution function. Thus, the complicated structural changes in the isotropic distribution with space and energy during the temporal evolution found by the solution of the space- and time-dependent electron Boltzmann equation in two-term approximation are convincingly verified by the Monte Carlo simulations.

The comparison between results of both approaches has been extended to the anisotropic distribution $f_1(z, U, t)$. As illustrative examples, results for the anisotropic distribution at an intermediate time of the respective spatiotemporal electron relaxation at $E = -6$ and -2 V/cm are shown in Figures 7a and 7b. Satisfactory agreement between the two-term Boltzmann

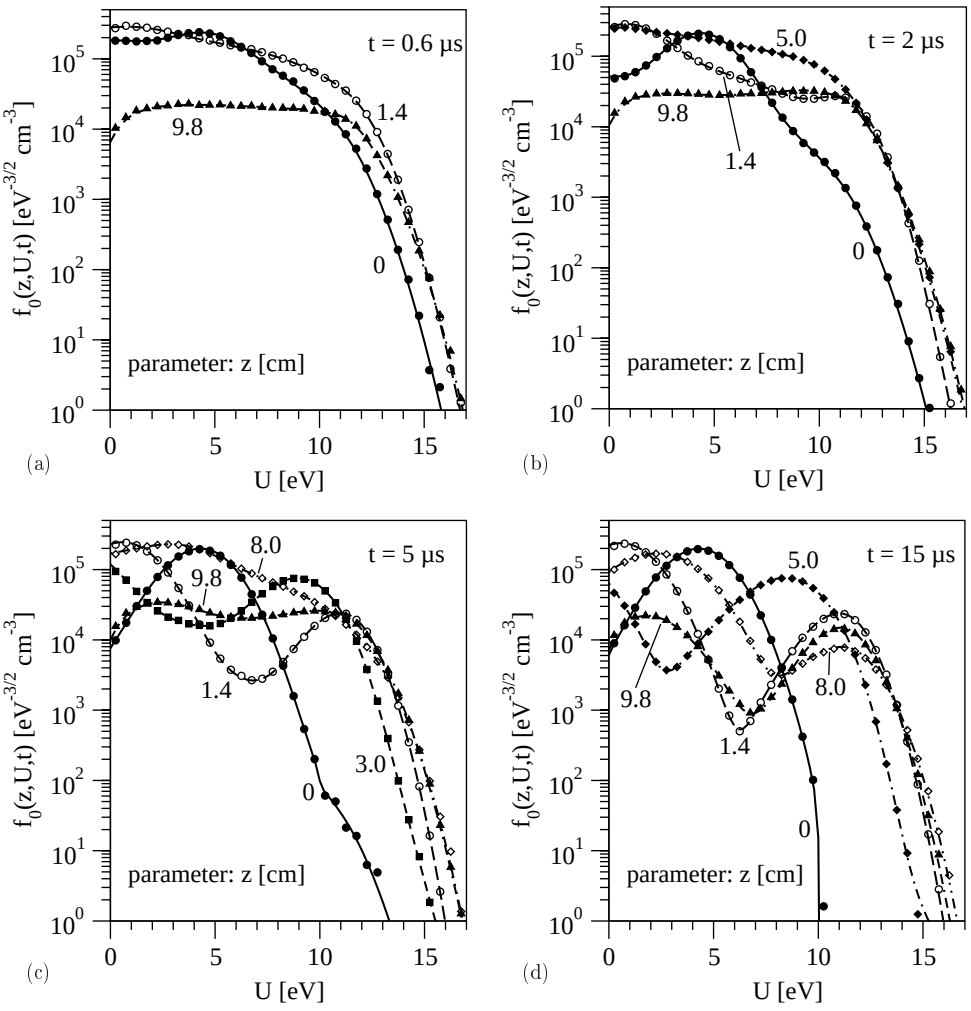

Fig. 5. Comparison between isotropic distributions $f_0(z, U, t)$ at various positions z obtained by Boltzmann (lines) and Monte Carlo (symbols) calculations for $E = -6$ V/cm at the times $t = 0.6$ (a), 2 (b), 5 (c) and 15 μs (d).

calculations and the Monte Carlo results is widely found. However, certain differences *e.g.* in the region of lower energies at $z = 0$ and 1.4 cm in Figure 7b and less pronounced differences in the region of medium energies at $z = 1.4$ cm in Figure 7a occur. In any case, main characteristics of the anisotropic distribution evolution are obtained consistently by both approaches. Since negative values of the electric field have been used to describe the acceleration of the electron in the positive z direction toward the anode, the anisotropic distribution usually assumes positive function values. However, the anisotropic distribution at lower energies for $z = 0$ and 1.4 cm in Figure 7b becomes negative, as indicated by the minus signs in parentheses. This probably happens because the isotropic distribution $f_0(z, U, t)$ has a branch with an opposite slope ($\partial f_0/\partial U > 0$) in the low energy region and the associated term becomes the dominant contribution to the anisotropic distribution $f_1(z, U, t)$ (6) during the relaxation at $E = -2$ V/cm. This particular result of the Boltzmann calculations has been confirmed by the Monte Carlo simulations, while the magnitude of the function values of both approaches differ.

As is obvious from the comparison of Figures 7a and 5c for $E = -6$ V/cm and of Figures 7b and 6c for $E = -2$ V/cm, the requirement of a sufficiently small magnitude of the distribution anisotropy, involved in the two-term Boltzmann approximation, generally holds and, therefore, the magnitude of the distribution anisotropy is not responsible for the observed discrepancies at small z positions. Furthermore, falsifications of the Boltzmann calculation results owing to the quasi-stationary description of the distribution anisotropy are rather improbable at the considered later times of the relaxation processes. Thus, the differences primarily have to be attributed to the reduced accuracy of the determination of the distribution anisotropy in the Monte Carlo simulations. In that approach the isotropic distribution f_0 is simply obtained by a summation of the number of electrons, while the determination of the anisotropic distribution f_1 includes a summation of the direction cosine v_z/v of the electrons. The quantity v_z/v ranges from -1 to 1. Since the velocity distribution function is substantially isotropic close to the isotropic electron source at $z = 0$ occurring in the range of lower kinetic energies, main parts of the

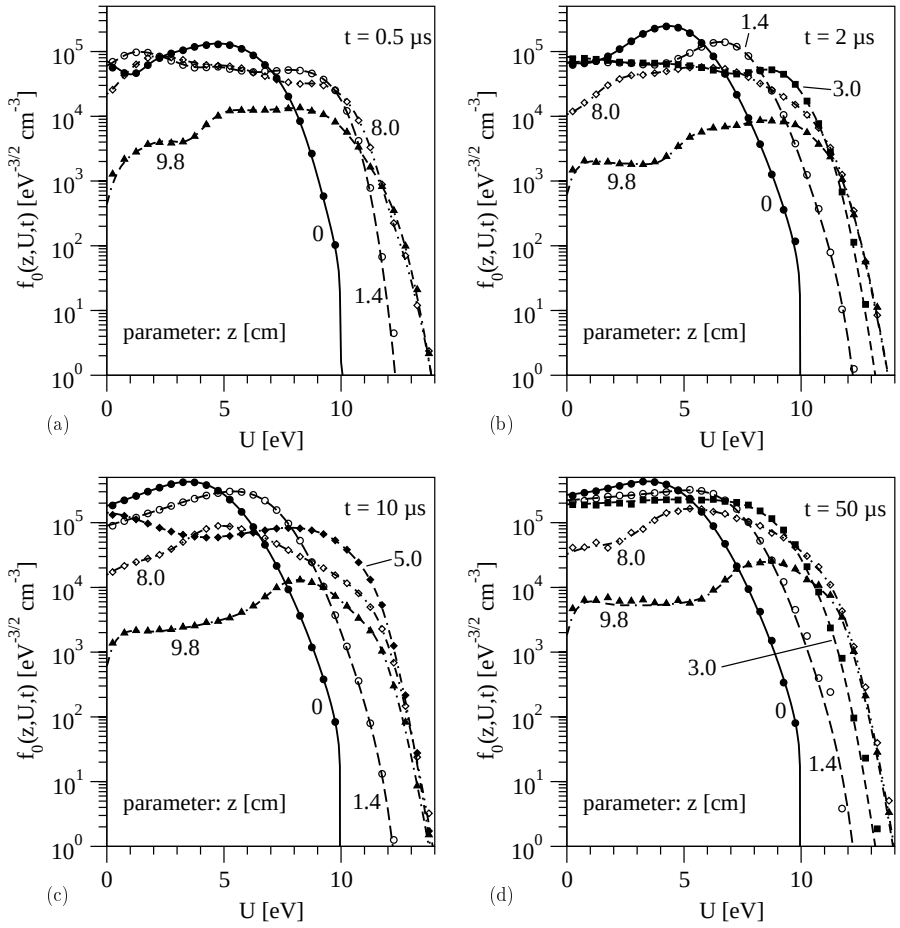

Fig. 6. Comparison between isotropic distributions $f_0(z, U, t)$ at various positions z obtained by Boltzmann (lines) and Monte Carlo (symbols) calculations for $E = -2$ V/cm at the times $t = 0.5$ (a), 2 (b), 10 (c) and 50 μs (d).

summation over v_z/v at these energies compensate for each other and it becomes difficult to determine the very small anisotropic distribution $f_1(z, U, t)$ with sufficient accuracy. In particular, this holds at the case of the low electric field magnitude.

Concerning the macroscopic quantities of the electrons the spatiotemporal evolution of the density $n_e(z, t)$, the mean energy $u_m(z, t)$ as well as the particle flux density $j_z(z, t)$ and the energy flux density $j_{ez}(z, t)$ is subsequently discussed. In Figure 8 results for these macroscopic quantities as a function of the space coordinate z are shown at different times of the relaxation course related to $E = -6$ V/cm. The lines display the Boltzmann calculation results, while the results obtained by the Monte Carlo simulation are represented by the symbols. The same line styles and symbol types have been employed to mark correlated results of the different macroscopic quantities.

The excellent agreement between the results of both approaches for the electron density (Fig. 8a) and mean energy (Fig. 8b) is apparent. It simply reflects the very good agreement found for the isotropic distribution $f_0(z, U, t)$ (Fig. 5), because both quantities are averages of it according to relations (7) and (8). The particle flux density (9) and energy flux density (10) are related to the anisotropic distribution $f_1(z, U, t)$. Although certain differences have been found for $f_1(z, U, t)$, the results for the related macroscopic quantities obtained by Boltzmann and Monte Carlo calculations are in quite good conformity, as can be seen from Figures 8c and 8d.

The activation of the spatiotemporal relaxation process by switching the electric field E from -2 to -6 V/cm leads initially to an increase of the particle and energy flux density (Figs. 8c and 8d), because the larger power input from the electric field increases the mean transport velocity of electrons and their energy transport velocity in the z direction. Thus, the spatial structure of the electron density (Fig. 8a) is transported from the cathode side to the anode, where about 64% of the electrons are absorbed. A continuous electron inflow I_s of 2×10^{12} cm^{-2} s^{-1} takes place at the cathode side. The released source electrons enforce a different spatial pattern after the abrupt increase of the magnitude of the field. The complex structural change of the electron density starts at the cathode side and propagates towards the anode. A similar change of the structure is found for the mean energy (Fig. 8b) and the energy flux density (Fig. 8d). When approaching the time-independent state after about 15 μs, the flux density has to decrease to the constant value prescribed by the

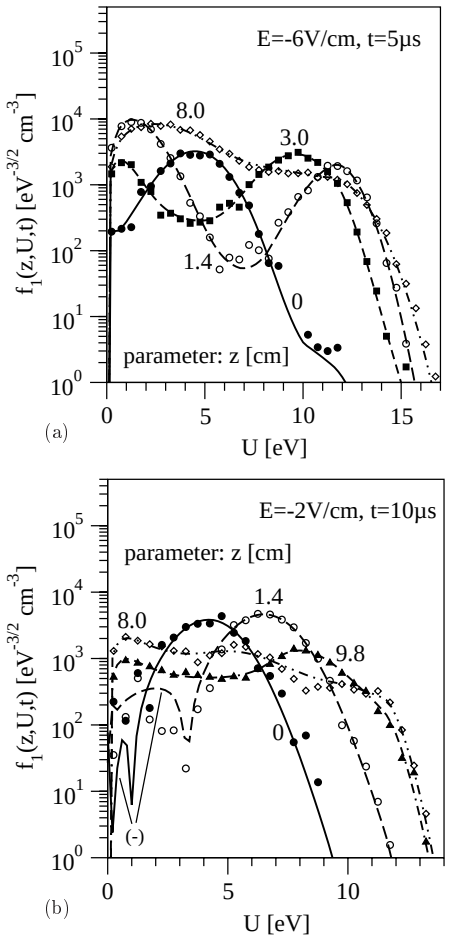

Fig. 7. Anisotropic distributions $f_1(z, U, t)$ at various positions z obtained by Boltzmann (lines) and Monte Carlo (symbols) calculations for $E = -6$ V/cm at $t = 5$ μs (a) and for $E = -2$ V/cm at $t = 10$ μs (b).

electron source. The time-independent state is additionally characterized by almost spatially periodic structures of the density, mean energy and energy flux density of the electrons resulting from the action of the field acceleration and the electron backscattering in inelastic collision processes. The structures are slightly damped towards the anode mainly because of the power loss in elastic collisions.

The corresponding results for the spatiotemporal relaxation at $E = -2$ V/cm are represented in Figure 9. Again, the Boltzmann and Monte Carlo calculation results for the density (Fig. 9a) and mean energy (Fig. 9b) of the electrons agree very well, while sufficient conformity is found for the particle flux density (Fig. 9c) and the energy flux density (Fig. 9d). Considering the results for the flux densities at $E = -2$ V/cm and those at -6 V/cm (Figs. 8c and 8d), it becomes obvious that the statistical fluctuations of the Monte Carlo results are more pronounced at $E = -2$ V/cm, although more electrons are usually involved at that electric field strength. The total number of electrons included in the spatiotemporal relaxation amounted to about 34×10^6 when approaching steady state at $E = -2$ V/cm, while about one third of this electron number is ultimately involved at $E = -6$ V/cm.

The spatiotemporal relaxation triggered by the sudden change of the electric field E from -6 to -2 V/cm at $t = 0$ processes rather differently from the reverse one. Now, the reduced power input from the field and the initially predominant depopulation of energetic electrons owing to inelastic collisions lead to a slower mean transport velocity of the electrons in z direction. The pronounced spatial structures of the density, mean energy and energy flux density at the beginning (shown in Figs. 8a, 8b and 8d at $t = 15$ μs) merge in the early phase of the relaxation, as is obvious from Figures 9a, 9b and 9d, respectively. Then, a reformation of the spatial structure of these quantities starts at the cathode side and the resulting structural change propagates towards the anode. This finding is mirrored well in the behaviour of particle flux density (Fig. 9c). The time-independent state is reached not until about 50 μs, *i.e.*, about three times later than the steady state related to the relaxation at $E = -6$ V/cm.

4 Concluding remarks

The spatiotemporal relaxation of the electron component in spatially inhomogeneous column-anode plasma regions of glow discharges between plane electrodes has successfully been studied by means of the solution of the space- and time-dependent Boltzmann equation in two-term approximation and by corresponding Monte Carlo simulations. A realistic relaxation model has been elaborated that allows the direct comparison between results obtained by both approaches. In the framework of the relaxation model, plasmas acted upon by a constant electric field and sustained by a continuous inflow of electrons at the cathode side are considered. The spatiotemporal electron relaxation starts from steady-state at a given field and is triggered by an instantaneous change of the electric field strength, while keeping the inflow of source electrons constant. The temporal reformation of spatial plasma structures in the velocity distribution function and in related macroscopic quantities of the electrons has been followed until approaching the time-independent state associated to the changed field strength.

The spatiotemporal relaxation of electrons in argon plasmas has been analyzed for electric fields typical of the column region of glow discharges. The magnitude of the electric field has been found to have a remarkable influence on the relaxation behaviour. The relaxation progresses in two phases controlled by different mechanisms. When increasing the electric field strength, the enlarged power input causes an increase of electrons with higher kinetic energy and tends to homogenize the distribution function in wide regions of the plasma. During the further temporal evolution pronounced, spatially periodic structures in the distribution function and essential macroscopic quantities are generated as a result of the enlarged impact of the inelastic collision processes. On the other hand, a decrease of the field leads to a mergence of the spatial plasma structures in the beginning of the relaxation. This mergence

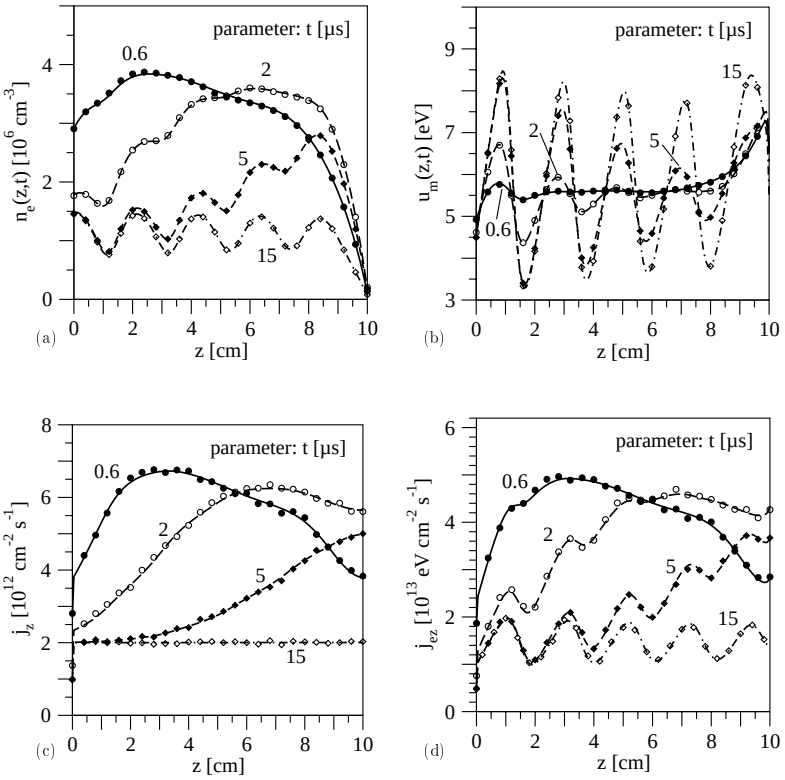

Fig. 8. Densities (a), mean energies (b), particle flux densities (c) and energy flux densities (d) of the electrons as a function of the space coordinate z obtained by Boltzmann (lines) and Monte Carlo (symbols) calculations for $E = -6$ V/cm at the times $t = 0.6$, 2, 5 and 15 μs.

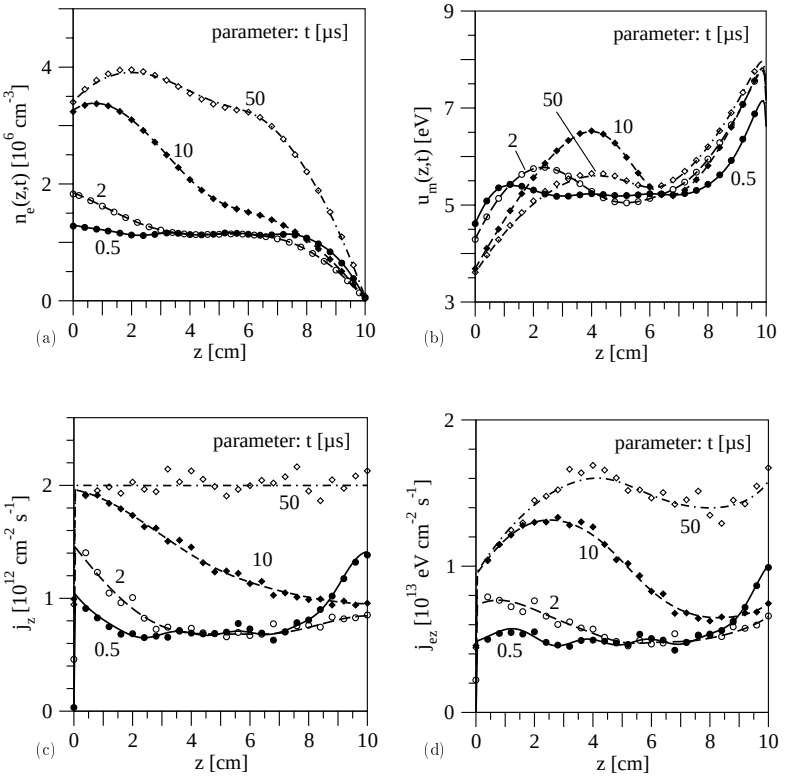

Fig. 9. Densities (a), mean energies (b), particle flux densities (c) and energy flux densities (d) of the electrons as a function of the space coordinate z obtained by Boltzmann (lines) and Monte Carlo (symbols) calculations for $E = -2$ V/cm at the times $t = 0.5$, 2, 10 and 50 μs.

results mainly from the interplay of the electron motion and action of inelastic collision processes. Then, new, but weaker spatial structures are formed because the larger effect of the elastic collisions leads to a stronger spatial damping. In any case, the formation of the spatial structures is induced by the continuous electron inflow at the cathode side and the spatial variations propagate towards the anode with a speed which is approximately given by the mean transport velocity.

The comparison between results obtained by solving the electron Boltzmann equation and by Monte Carlo simulation reveals very good agreement for the isotropic part of the velocity distribution function and the macroscopic quantities during the transient process as well as in steady-state. The results of the anisotropic distribution functions show satisfactory conformity, where some remaining discrepancies can be attributed to difficulties of the Monte Carlo approach to obtain the anisotropic distribution close to the isotropic electron source and at energies where the velocity distribution function is essentially isotropic. The complex mechanisms of the spatiotemporal electron relaxation found in former and present Boltzmann equation studies are impressively confirmed by the particle simulation approach. Thus, the two-term treatment of the electron kinetic equation is appropriate to study a variety of spatiotemporal relaxation processes related to basic research and technologically relevant plasmas as well.

When considering the performance of both approaches, much better efficiency of the Boltzmann equation method has been found. At the same time it became clear that Monte Carlo simulations will become increasingly adequate to study spatiotemporal relaxation processes with the anticipated further increase of computational speed in next years.

Z. Donkó thanks T. Šimko for useful discussions on the Monte Carlo simulation technique. This work was in part financially supported through the grants of OTKA-T-25989 and OTKA-T-34156.

References

1. S.D. Rockwood, Phys. Rev. A **8**, 2348 (1973)
2. J. Wilhelm, R. Winkler, J. Phys. Coll. **40** (C7 Suppl. 7), 251 (1979)
3. W.L. Morgan, B.M. Penetrante, Comput. Phys. Commun. **58**, 127 (1990)
4. E. Estocq, G. Delouya, J. Bretagne, Appl. Phys. B **56**, 209 (1993)
5. D. Loffhagen, R. Winkler, J. Comput. Phys. **112**, 91 (1994)
6. D. Loffhagen, R. Winkler, J. Phys. D: Appl. Phys. **29**, 618 (1996)
7. C.A. Hall, J.J. Lowke, J. Comput. Phys. **19**, 297 (1975)
8. V.A. Shveigert, Sov. J. Plasma Phys. **15**, 714 (1989)
9. J.V. DiCarlo, M.J. Kushner, J. Appl. Phys. **66**, 5763 (1989)
10. T.C. Paulick, J. Appl. Phys. **67**, 2774 (1990)
11. C. Busch, U. Kortshagen, Phys. Rev. E **51**, 280 (1995)
12. F. Sigeneger, R. Winkler, Contrib. Plasma Phys. **36**, 551 (1996)
13. D. Uhrlandt, R. Winkler, J. Phys. D: Appl. Phys. **29**, 115 (1996)
14. Y. Yang, H. Wu, J. Appl. Phys. **80**, 3699 (1996)
15. L.L. Alves, G. Gousset, C.M. Ferreira, Phys. Rev. E **55**, 890 (1997)
16. G. Petrov, R. Winkler, J. Phys. D: Appl. Phys. **30**, 53 (1997)
17. S.C. Arndt, D. Uhrlandt, R. Winkler, Plasma Chem. Plasma Process. **21**, 175 (2001)
18. W.J. Goedheer, P.M. Meijer, J. Nucl. Mater. **200**, 282 (1993)
19. M.O.M. Mahmoud, M. Yousfi, J. Appl. Phys. **89**, 5935 (1997)
20. D. Loffhagen, R. Winkler, J. Phys. D: Appl. Phys. **34**, 1355 (2001)
21. H.R. Skullerud, J. Phys. D: Appl. Phys. **1**, 1567 (1968)
22. G.L. Braglia, Physica **92C**, 91 (1977)
23. J.P. Boeuf, L.C. Pitchford, IEEE Trans. Plasma Sci. **19**, 286 (1991)
24. A. Fiala, L.C. Pitchford, J.P. Boeuf, Phys. Rev. E **49**, 5607 (1994)
25. A. Bogaerts, R. Gijbels, W.J. Goedheer, J. Appl. Phys. **78**, 2233 (1995)
26. Z. Donkó, K. Rózsa, R.C. Tobin, J. Phys. D: Appl. Phys. **29**, 105 (1996)
27. T. Šimko, V. Martišovitš, J. Bretagne, G. Gousset, Phys. Rev. E **56**, 5908 (1997)
28. K. Maeda, T. Makabe, N. Nakano, S. Bzenić, Z.Lj. Petrović, Phys. Rev. E **55**, 5901 (1997)
29. S. Bzenić, Z.Lj. Petrović, M. Raspopović, T. Makabe, Jpn. J. Appl. Phys. **38**, 6077 (1999)
30. A. Bogaerts, R. Gijbels, W. Goedheer, J. Anal. At. Spectrom. **16**, 750 (2001)
31. R. Winkler, G. Petrov, F. Sigeneger, D. Uhrlandt, Plasma Sources Sci. Technol. **6**, 118 (1997)
32. R. Winkler, J. Wilhelm, V. Schüller, Beitr. Plasma Phys. **10**, 51 (1970)
33. H. Leyh, D. Loffhagen, R. Winkler, Comput. Phys. Commun. **113**, 33 (1998)
34. D.U. von Rosenberg, *Methods for the Numerical Solution of Partial Differential Equations* (American Elsevier, New York, 1969)
35. J.P. Boeuf, E. Marode, J. Phys. D: Appl. Phys. **15**, 2169 (1982)
36. S. Longo, Plasma Sources Sci. Technol. **9**, 468 (2000)
37. B.M. Penetrante, J.N. Bardsley, L.C. Pitchford, J. Phys. D: Appl. Phys. **18**, 1087 (1985)
38. M. Yousfi, A. Hennad, A. Alkaa, Phys. Rev. E **49**, 3264 (1994)
39. A.V. Phelps (2001), `ftp://jila.colorado.edu/collision_data/`
40. F. Sigeneger, R. Winkler, Plasma Chem. Plasma Process. **17**, 1 (1997)